Molecular Biotechnology (2022) 64:199–212
https://doi.org/10.1007/s12033-021-00406-8

ORIGINAL PAPER

METTL14-Mediated miR-30c-1-3p Maturation Represses the Progression of Lung Cancer via Regulation of MARCKSL1 Expression

Fei Li[1] · Jing Zhao[2] · Lei Wang[1] · Yantong Chi[1] · Xiaori Huang[1] · Wei Liu[1]

Received: 31 May 2021 / Accepted: 20 September 2021 / Published online: 29 September 2021

Abstract

Lung cancer (LC) is a pulmonary malignant tumor with extremely low 5-year survival rate. N6-methyladenosine (m6A) is confirmed to regulate diverse pathophysiological processes including cancers. Methyltransferase-like 14 (METTL14) is an important RNA methyltransferase in m6A modification. However, researches on the regulatory mechanism of METTL14 on LC progression are relatively rare. Tumor xenograft experiment was conducted to investigate the effect of METTL14 on LC in vivo. The relative expression of METTL14, miR-30c-1-3p, and myristoylated alanine-rich C kinase substrate-like protein-1 (MARCKSL1) in LC tissues and/or cell lines was determined using qRT-PCR. Western blot assay was used to measure the protein levels of METTL14 and MARCKSL1 in tumor xenograft model and/or LC cell lines. MTT, wound healing, and transwell assays were performed to detect LC cell viability and metastasis. RNA immunoprecipitation assay and qRT-PCR were used to verify the effects of METTL14 on pri-miR-30c-1-3p. The relationship between miR-30c-1-3p and MARCKSL1 was confirmed by the dual-luciferase reporter assay. METTL14 was remarkably downregulated in LC tissues and cell lines. METTL14 mediated the maturation of miR-30c-1-3p. The overexpressed METTL14 and overexpressed miR-30c-1-3p suppressed the cell viability and metastasis in LC. Meanwhile, the increased METTL14 also repressed the growth of tumor xenograft in vivo. In addition, MARCKSL1 was confirmed to be the target gene of miR-30c-1-3p. High expression of MARCKSL1 and low expression of miR-30c-1-3p reversed the suppressive effects of METTL14 overexpression on cell viability and metastasis. METTL14 promoted the maturation of miR-30c-1-3p and mediated MARCKSL1 expression to inhibit the progression of LC. This study may provide a new insight for the LC clinical therapy.

Keywords Lung cancer · METTL14 · N6-methyladenosine · miR-30c-1-3p · MARCKSL1

Introduction

Lung cancer (LC) is a kind of pulmonary malignant tumor with higher lethality than the four common cancers (colorectal, breast, pancreas, and prostate cancers) [1, 2], typically originates from the excessive hyperplasia of cancer cells [1]. With no obvious clinical symptoms in early stage and the limitations of the current diagnostic-methods, LC is typically discovered at an advanced stage [3]. Currently, although therapies for advanced LC patients such as nanomedicine and immunotherapy have made great progress in the last few years [4, 5], there are still no efficient therapies to improve the 5-year survival rate (less than 5%) [6]. Therefore, exploring the potential regulatory mechanism of LC and developing promising targets are urgent for treating LC.

N6-methyladenosine (m6A) modification is one of the 100 identified structurally distinct chemical modifications that occurs in eukaryotes to influence the activity and stability of mRNA, rRNA, and miRNA [7–10]. The procedures of m6A modification need three kinds of enzymes to work together collaboratively, including RNA methyltransferase (writers) complex [Wilm's tumor 1 associated protein (WTAP), methyltransferase-like 3 (METTL3), methyltransferase-like 14 (METTL14), and vir-Like m6A methyltransferase associated (KIAA1429)] [11–14], RNA demethylases

✉ Fei Li
lifei364@126.com

[1] Department of Pulmonary and Critical Care Medicine, People's Hospital of Rizhao, No. 126, Tai'an Road, Donggang District, Rizhao 276800, Shandong, China

[2] Outreach Department, People's Hospital of Rizhao, Rizhao 276800, Shandong, China

(erasers) including alkylation repair homolog protein 5 (ALKBH5) and fat-mass and obesity-associated protein (FTO) [15, 16], and reader proteins (readers) including heterogeneous nuclear ribonucleoprotein (HNRNPC) and YTH domain-containing family protein 1/2/3 (YTHDF1/2/3) [17, 18]. m6A modification is reversible, which is added by methyltransferase complex and removed by m6A demethylases [10]. The influence of m6A in RNA stability is dependent on m6A readers [11]. m6A modification is important for mammals and participates in many biological processes, including spermatogenesis and embryonic development [19–21], circadian period [22], DNA damage [23], hematopoietic stem cells [24], and tissue homeostasis [25]. As for tumor biology, m6A modification exerts its role in tumorigenesis, proliferation, and metastasis [12, 26, 27]. Jin et al. have revealed that METTL3/m6A modification elevates the activity of YAP, and aggravates the malignant phenotypes of non-small-cell LC (NSCLC) [12]. Du et al. have confirmed that YTHDF2 can "read" the m6A of mps one binder kinase activator 3B (MOB3B), repress the expression of MOB3B, and eventually promote the development of prostate cancer (PC) [26]. Strick et al. explored the association between m6A "erasers" (ALKBH5 and FTO) and the overall survival of patients with clear cell renal cell carcinoma (ccRCC), and demonstrated that the decreased ALKBH5 and FTO are strongly correlated with the poor prognosis of ccRCC patients [27]. Additionally, RNA methyltransferase such as WTAP, METTL3, and KIAA1429, RNA demethylases such as ALKBH5 and FTO, and reader proteins have been confirmed to be closely associated with devastating pulmonary diseases including NSCLC and lung adenocarcinoma (LAD) [28–33]. Notably, as a member of RNA methyltransferase, METTL14 is observed to downregulate in bladder cancer (BC) [11], colorectal cancer (CRC) [34], and LAD [35]. However, the detailed regulatory mechanism of METTL14 on LC progression remains unclear.

Mature microRNAs (miRNAs) with 16–25 nucleotides in length can regulate gene expression by translational suppression or degradation of their target mRNAs [36]. It is widely known that m6A modification makes valuable contributions on the formation of mature miRNAs, thereby regulating the expression of downstream target mRNAs [37–39]. For instance, METTL3/m6A modification accelerates pri-miR-126-5p to form miR-126-5p, whereas the maturation of miR-126-5p further targets PTEN to affect the progression of ovarian cancer (OC) [40]. Similarly, in breast cancer (BRC), METTL3 affects the expression miR-let-7g, and interacts with HBXIP to promote tumorigenesis [37]. Notably, METTL14/m6A is also reported to be involved in primary miRNA processing in human diseases, such as METTL14-miR-126 in hepatocellular carcinoma (HCC) [38], METTL14-miR-146a-5p in BRC [39], METTL14-miR-375 in CRC [41], and METTL14-miR-19a in atherosclerosis (AS) [42]. Notably, miR-30c-1-3p showed crucial role in the tumorigenesis of melanoma, meningioma, and PC [43–45]. More importantly, Wu et al. found that increased expression of the matured miR-30c-1-3p significantly inhibited pulmonary fibrosis [46]. However, researches on whether METTL14/m6A is involved in the maturation of miR-30c-1-3p, and the matured miR-30c-1-3p is associated with LC tumorigenesis are relatively rare. In addition, as an oncogene, MARCKSL1 is commonly targeted by miRNAs to exhibit its promoting role in human cancers, including miR-21 in PC [47], miR-140-3p in BRC [48], and miR-34c-3p in osteosarcoma [49]. More importantly, a recent study conducted by Liang et al. has uncovered that MARCKSL1 is upregulated in LAD tissues and promotes LAD progression through regulation of epithelial–mesenchymal transition (EMT) [50]. Nevertheless, the possible role of MARCKSL1 in LC and whether miR-30c-1-3p interacts with MARCKSL1 on the occurrence and development of LC remains to be further explored.

In this study, we hypothesize that METTL14/m6A mediates the maturation of miR-30c-1p, and further targets MARCKSL1 to affect LC progression. Based on this assumption, the possible roles of METTL14 on LC cell viability, metastasis, and pri-miR-30c-1-3p, as well as the interactions among METTL14, miR-30c-1-3p, and MARCKSL1 on the tumorigenesis of LC were investigated. Our findings that a tumorigenic mechanism mediated by m6A modification involves in METTL14 and the miR-30c-1-3p/MARCKSL1 axis may provide underlying molecular targets for the treatment of LC in the future clinical application.

Materials and Methods

LC Samples

A total of 75 LC patients who received histological examination were recruited in our hospital from June 2017 to July 2019. All the participators had not received any treatments before surgery. The LC tissues and corresponding adjacent normal tissues (ANT) were collected by surgical operation. The collected tissues were immediately stored in liquid nitrogen for the subsequent experiments. This study was performed in line with the principles of the Declaration of Helsinki. The present study was approved by Ethics Committee of Peoples Hospital of Rizhao, and the relevant informed consents were written by each patient.

Cell Culture, Reagents, and Transfection

Four LC cell lines (PC-9, H1975, A549, and H1299) and a human normal lung epithelial cell line BEAS-2B procured from American Type Culture Collection (Manassas,

VA, USA) were cultured in DMEM containing 10% FBS at 37 °C with 5% CO_2. MARCKSL1 overexpression vector (pcDNA-MARCKSL1), pcDNA-MELLT14 and the corresponding negative control (pcDNA-NC), small hairpin targeting MELLT14 (sh-MELLT14) and sh-NC, as well as miR-30c-1-3p mimics/miR-NC and miR-30c-1-3p inhibitor/inhibitor NC (all from VectorBuilder, Guangzhou, China) were co-transfected with A549 and H1299 cells. The transfection procedures were conducted using Lipofectamine™ 3000 Transfection Reagent (Invitrogen, Carlsbad, CA, USA).

Analysis for Quantitative Real Time PCR (qRT-PCR) and RNA m6A Quantification

Total RNA was extracted from LC tissues and cell lines using Trizol Reagent (Invitrogen). The cDNA was synthesized using RevertAid H Minus First Strand cDNA Synthesis Kit (Thermo Fisher Scientific, Waltham, MA, USA). Afterward, cDNA was used to perform qRT-PCR analysis with DyNAmo Flash SYBR Green qPCR Kit (Thermo Fisher Scientific). The $2^{-\Delta\Delta C_t}$ method was utilized to calculate the relative expression. GAPDH and U6 were used as the internal controls.

The m6A RNA methylation assay kit (ab185912; Abcam, Cambridge, UK) was used for the quantification of RNA m6A as previously described [39, 41]. Briefly, pcDNA-NC (2 µl), pcDNA-METTL14 (2 µl), and the aforementioned total RNA (200 ng) were added to a 96-well plate. Afterward, 50 µl of diluted capture antibody, detection antibody, and diluted enhancer solution were added into each well following the manufacturer's protocol. Signaling was detected after adding 100 µl diluted developer solution and stop solution to each well within 2 to 10 min using a microplate reader (Molecular Devices, Shanghai, China) at 450 nm. A standard curve was then used to calculate relative m6A content.

Western Blot Assay

Antibodies used for western blotting including the primary antibodies (METTL14, MARCKSL1, and GAPDH) and the HRP-conjugated secondary antibody were all procured from Abcam. The procedures were performed as follows: proteins from the LC cell lines (A549 and H1299) and xenografted mice tissues were initially lysed with RIPA buffer. We then made detection for protein concentrations using a BCA Protein Assay Kit (Thermo Fisher Scientific). The protein samples (40 µg) were separated by sodium dodecyl sulfate-polyacrylamide gel electrophoresis on 10% gels and electro-blotted onto a polyvinylidene fluoride membrane. The membrane was blocked with 5% skim milk in Tris-buffered saline containing 0.1% Tween 20 (TBST) for 1 h at room temperature, and incubated with the relevant primary antibodies (1:1000) at 4 °C for overnight. After three washes with TBST, the membrane was incubated with the secondary antibody (1:5000) for 1 h at room temperature. GAPDH was used as the internal control. Immunoblottings were visualized using an ECL detection kit (Amersham Biosciences, Sweden).

Wound Healing Assay

The transfected A549 and H1299 cells (1×10^5 cells/µl) were plated in 12-well dishes and grown to nearly 100% confluence. Subsequently, a sterile pipette tip (10 µl) was used for creating the wounds. After that, the cells were incubated for 24 h in a serum-free medium. Then, the cells were washed three times with phosphate-buffered saline (PBS) to wash away the floating cells. At 0 h and 24 h, photos were taken under a light microscope (Olympus Corporation, Guangdong, China) and analyzed with ImageJ software [National Institutes of Health (NIH), Bethesda, MD, USA]. The relative migration (%) was calculated as (original gap distance − gap distance at 24 h)/original gap distance × 100, and normalized to that of the corresponding control group.

MTT Assay

After transfection, A549 and H1299 cells (2×10^3) were transferred into 96-well plates. At the time point of 0, 24, 48, 72, and 96 h, respectively, 20 µl MTT (Beyotime, Beijing, China) was added to incubate 2 h at 37 °C. The absorbance values were detected by a microplate reader (Molecular Devices) at the wavelength of 450 nm.

Transwell Assay

The upper chamber of Transwell inserts was pre-coated with Matrigel (BD Biosciences) at 37 °C for 30 min according to the manufacturer's instructions. The transfected A549 and H1299 cells (2×10^5) were re-suspended in serum-free DMEM and then transferred onto the Matrigel coated upper chamber, and DMEM containing 10% FBS was added to the lower chamber. After incubation for 24 h at 37 °C, the non-invaded cells in the upper chamber were scraped off with cotton swabs, and the cells that invaded the lower inserts were fixed with 90% ethanol and stained with 0.5% crystal violet at 37 °C for 15 min. The stained cells were imaged and counted in five random fields under an inverted light microscope. The number of invading cells was calculated by normalizing to that of the corresponding control group.

Tumor Xenograft Experiments

A total of 10 BALB/c nude mice (4–5 weeks, 22–24 g; Ese-Bio, Shanghai, China) were assigned into the pcDNA-NC

group and pcDNA-METTL14 group ($n=5$) ad libitum. The mice were initially anesthetized by intraperitoneal injection of 50 mg/kg pentobarbital sodium. A549 cells transfected with pcDNA-METTL14 or pcDNA-NC were washed with PBS and detached with 0.25% trypsin. After centrifugation, the cell pellet was re-suspended with normal saline and dispersed into a single-cell suspension. The cells (1×10^6) were re-suspended in normal saline and mixed with 25% Matrigel matrix (50 µl) at a 1:1 ratio and subcutaneously injected into the right groin of the mice. The tumor volume was measured using the following formula: V (volume) = 1/2 [A (tumor length) B (tumor width)]^2. Four weeks later, the mice were sacrificed and the tumors were collected and weighed. The present study was approved by the Institutional Animal Care and Use Committee of our hospital.

RNA Immunoprecipitation Assay

An RNA immunoprecipitation (RIP) assay was performed with a Magna RIP Kit (Millipore, Billerica, MA, USA) in accordance with the manufacturer's protocol. Cells were lysed in RIP lysis buffer, and then, 100 µl whole-cell extract was incubated with magnetic beads conjugated with anti-DGCR8 (1:100; Abcam) or IgG (1:100; Abcam) at 4 °C for 6 h. Thereafter, the beads were incubated with proteinase K with shaking to remove protein. The coprecipitated RNAs were extracted by phenol–chloroform–isopentyl alcohol (125:24:1) and subjected to qRT-PCR.

Magna Me-RIP m6A Kit (Millipore) was used for the m6A RNA binding assay. The cells were digested with DNase I and ultrasonicated for 10 s to disrupt RNA. The magnetic beads were incubated with anti-m6A (1:500; Abcam) or IgG (1:500; Abcam) at room temperature for 1 h. The antibody–beads complex, RIP immunoprecipitation buffer, and RNA fragments were fully mixed, and then incubated together overnight at 4 °C. The protein–RNA complex was digested by proteinase K, and then the RNA was extracted and subjected to qRT-PCR.

Dual-Luciferase Reporter (DLR) Assay

The underlying binding site between miR-30c-1-3p and MARCKSL1 was predicted using miRDB software (http://mirdb.org/) and verified by DLR assay. In brief, the fragments of MARCKSL1 containing miR-30c-1-3p binding site [including wild type (WT) and mutant type (MUT)] were initially inserted into pGL3 vector to establish the recombinant reporter plasmids. Subsequently, A549 cells (3000 cells/well) were co-transfected with miR-30c-1-3p mimics/miR-NC, and MARCKSL1 wt or MARCKSL1 mut using Lipofectamine 3000 (Invitrogen) to incubate for 48 h at 37 °C. After that, the luciferase activity was analyzed using a dual-luciferase reporter gene assay system (Promega Corporation).

Statistical Analysis

Data in this study are shown as means ± SD. SPSS 23.0 software was used to perform statistical analyses. Student's t-test, one-way ANOVA followed by Tukey's multiple comparisons test, and two-way ANOVA followed by Sidak's multiple comparisons test were used to analyze the experimental data in this study. The survival curves are compared with log-rank test. Pearson's correlation was used for analysis the linear correlation in tumor tissues of LC patients. Significance difference was considered when $P<0.05$. All in vitro experiments were performed in triplicate.

Results

Decreased METTL14 is Identified in LC Tissues and Cells

We initially investigated the expression of METTL14 in LC tissues based on the databases of The Cancer Genome Atlas (TCGA) and Gene Expression Omnibus (GEO). As shown in Fig. 1A, B, reduction of METTL14 was observed in LC tissues compared with the normal tissues ($P<0.01$). In addition, Kaplan–Meier analysis indicated that relatively low expression of METTL14 was closely correlated with the poor survival rate in LC patients (Fig. 1C, logrank $P=0.0026$). We then detected METTL14 expression in clinical LC samples and cell lines. We found that METTL14 was downregulated in tumor tissues compared to that in ANT (Fig. 1D, $P<0.01$). Meanwhile, a decreased METTL14 was observed in LC cell lines in comparison to the BEAS-2B cells (Fig. 1E, $P<0.05$). A549 and H1299 cell lines were chosen for the subsequent experiments due to the relatively high expression of METTL14. In addition, the correlation between METTL14 expression and different clinical characteristics was also analyzed. As shown in Table 1, we found that high expression of METTL14 and low expression of METTL14 showed significant difference in TNM stage ($P=0.0184$) and tumor differentiation ($P=0.0258$).

Overexpressed METTL14 Inhibits the Cell Viability and Metastasis in LC

Next, the role of METTL14 on LC progression was explored. We overexpressed METTL14 via transfection of pcDNA-METTL14 into A549 and H1299 cells. As presented in Fig. 2A, METTL14 expression was significantly upregulated by pcDNA-METTL14 transfection ($P<0.01$). Similar patterns were observed in the data of METTL14

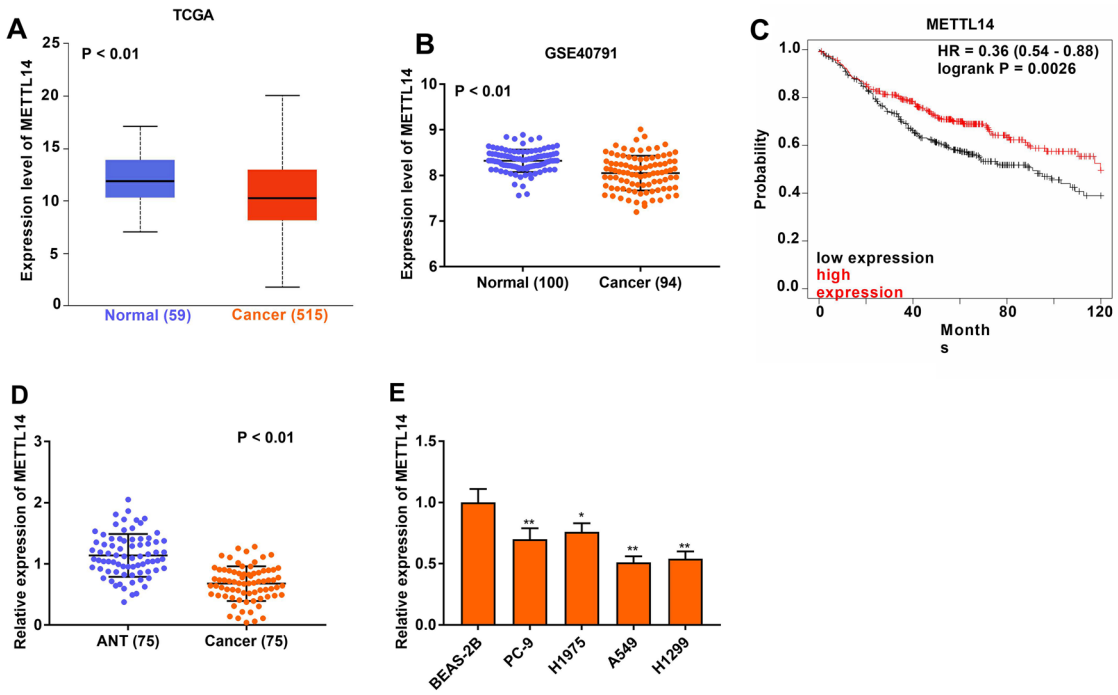

Fig. 1 Decreased METTL14 is identified in LC tissues and cells. **A** The expression of METTL14 in LC tissues was analyzed using TCGA database. $P<0.01$ vs. the normal tissues. **B** The expression of METTL14 in LC tissues was analyzed using GSE40791 cohort in GEO database. $P<0.01$ vs. the normal tissues. **C** The effect of different expression level of METTL14 on LC prognosis was analyzed using the platform of Kaplan–Meier Plotter. Logrank $P=0.0026$. **D** The expression of METTL14 in LC tissues ($n=75$) and adjacent normal tissues ($n=75$) was detected by qRT-PCR. $P<0.01$ vs. the adjacent normal tissues. **E** The expression of METTL14 in H1299, A549, PC-9, H1975, and BEAS-2B cells was detected by qRT-PCR. $^*P<0.05$, $^{**}P<0.01$ vs. the BEAS-2B cells group

Table 1 Correlation between METTL14 expression and different clinical characteristics

Characteristics	$N=75$ (%)	METTL14 expression		P value
		High ($n=41$)	Low ($n=34$)	
Gender				0.639
Male	46 (61.33%)	24	22	
Female	29 (38.67%)	17	12	
Age (years)				0.806
< 60	23 (30.67%)	12	11	
≥ 60	52 (69.33%)	29	23	
TNM stage				0.0184*
I–II	43 (57.33%)	29	14	
III–IV	32 (42.67%)	12	20	
Differentiation				0.0258*
Low	18 (24.0%)	5	13	
Moderate	46 (61.33%)	30	16	
High	11 (14.67%)	6	5	
Tumor size				0.165
< 5 cm	44 (58.67%)	27	17	
≥ 5 cm	31 (41.33%)	14	17	

protein level (Fig. 2B, P < 0.01). It is indicated that the formation of of m6A modification is positively associated with METTL14 level [11]. Therefore, m6A contents in A549 and H1299 cells were further measured and we found that the contents of m6A were increased by METTL14 overexpression (Fig. 2C, P < 0.05). Meanwhile, the results of wound healing, transwell invasion, and MTT assays demonstrated that the overexpressed METTL14 significantly repressed the migration, invasion, and viability of LC cells (Fig. 2D, F, P < 0.05).

Upregulation of METTL14 Suppresses the Growth of Tumor Xenograft In Vivo

The effect of METTL14 overexpression on the growth of tumor xenograft in vivo was also studied. As illustrated in Fig. 3A–C, injection of A549 cells transfected with pcDNA-METTL14 not only decreased tumor volume ($P<0.01$), but also reduced tumor weight ($P<0.01$), suggesting that the increased METTL14 repressed the growth of tumor xenograft. Furthermore, western blot assay revealed that the protein level of METTL14 in tumor tissues of mice was elevated after injection with pcDNA-METTL14 (Fig. 3D, P < 0.01).

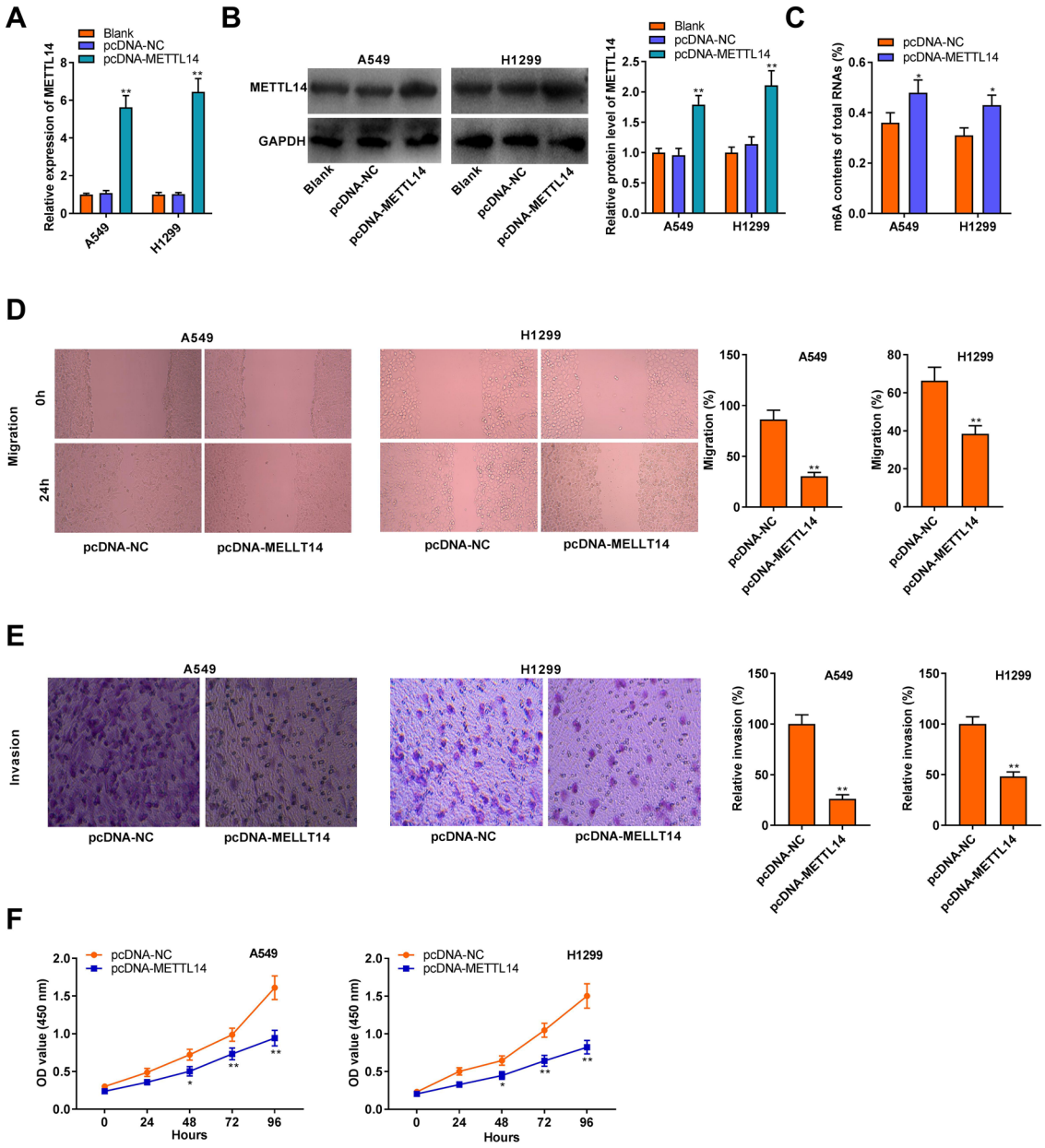

Fig. 2 Overexpressed METTL14 inhibits the cell viability and metastasis in LC. **A** The expression of METTL14 in LC cells after transfection of pcDNA-METTL14/NC was detected by qRT-PCR. **B** The protein level of METTL14 in LC cells after transfection of pcDNA-METTL14/NC was determined by western blot assay. **C** The m6A contents of total RNAs were detected using the m6A RNA methylation assay kit in METTL14 overexpressed LC cells. **D** The migration of LC cells was measured by wound healing assay. **E** The invasion of LC cells was measured by transwell assay. **F** The viability of LC was measured by MTT assay. *$P<0.05$, **$P<0.01$ vs. the pcDNA-NC group

METTL14-Mediated m6A Methylation Regulates the Processing of miR-30c-1-3p by DGCR8

In accordance with the analysis of LinkedOmics databases, a total of 50 miRNAs were found to be positively correlated with METTL14 in LC tissues (Supplement Fig. 1). We then investigated the expression of these miRNAs in LC cells after transfection of sh-METTL14/NC or pcDNA-METTL14/NC. The expression of METTL14 was downregulated by transfection of sh-METTL14, which implied that sh-METTL14 was transfected into A549 and H1299 cells successfully (Fig. 4A, $P<0.01$). As shown in Fig. 4B, we discovered that miR-30c-1-3p was significantly decreased by METTL14 deletion and increased by METTL14 upregulation ($P<0.01$). Subsequently, we applied DGCR8, the key enzyme in m6A modification that

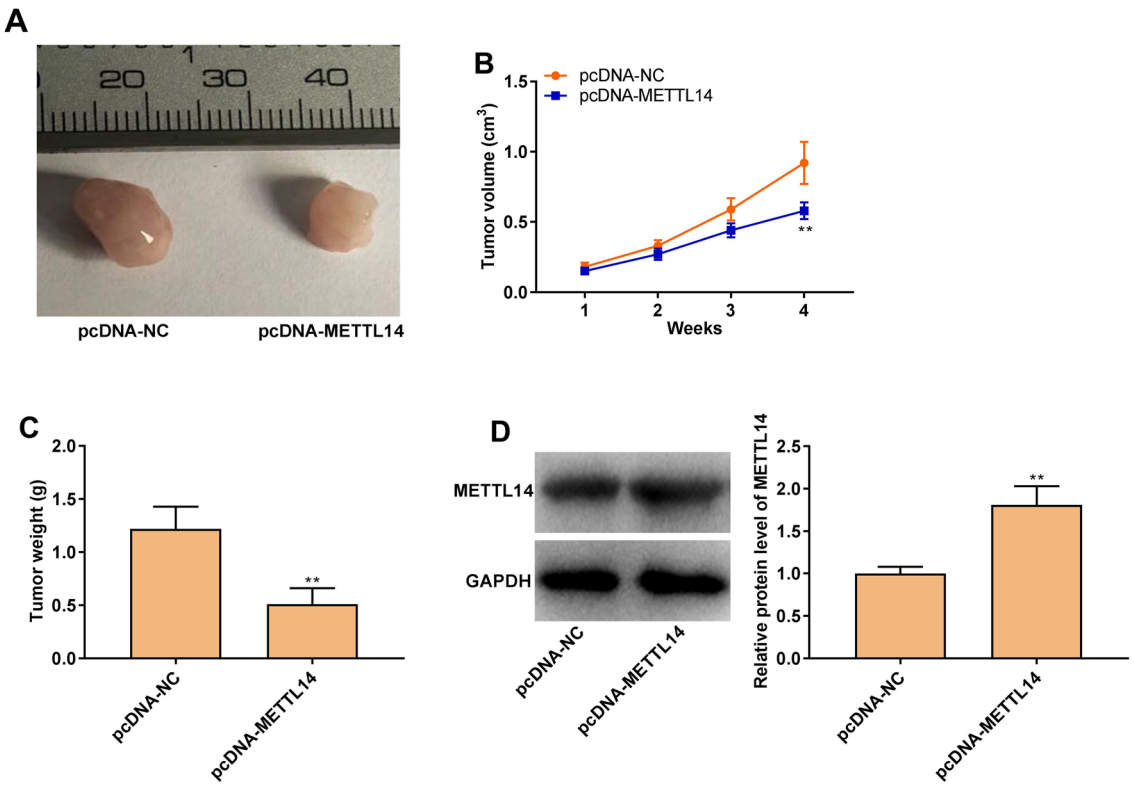

Fig. 3 Upregulation of METTL14 suppresses the growth of tumor xenograft in vivo. **A** The image of solid tumor after injection of pcDNA-METTL14/NC. **B** The tumor volume after injection of pcDNA-METTL14/NC. **C** The tumor weight after injection of pcDNA-METTL14/NC. **D** The protein level of METTL14 in tumor xenograft tissues injected with pcDNA-METTL14/NC was measured by western blot assay. $^{**}P < 0.01$ vs. the pcDNA-NC group

can promote pri-miRNA to form the mature miRNA, and m6A as antibodies, and then detected the m6A modification level of pri-miR-30c-1-3p by RIP and Me-RIP experiments. We discovered that pri-miR-30c-1-3p was significantly enriched in the pcDNA-METTL14 + DGCR8 and pcDNA-METTL14 + m6A groups compared to that in the pcDNA-NC + DGCR8 and pcDNA-NC + m6A groups, respectively (Fig. 4C, D, $P < 0.01$). In addition, we also found miR-30c-1-3p expression was reduced in tumor tissues by contrast to the ANT (Fig. 4E, $P < 0.01$), and there was a positive correlation between the expression of METTL14 and miR-30c-1-3p in LC tissues (Fig. 4F; $P < 0.01$, $r = 0.502$).

Overexpression of miR-30c-1-3p Inhibits the Cell Viability and Metastasis in LC

miR-30c-1-3p mimics/miR-NC or miR-30c-1-3p/inhibitor NC was transfected into A549 and H1299 cells to explore the function of miR-30c-1-3p on the tumorigenesis of LC. As illustrated in Fig. 5A, B, in both A549 and H1299 cells, miR-30c-1-3p was upregulated by transfection with miR-30c-1-3p mimics, and was downregulated after transfection of miR-30c-1-3p inhibitor ($P < 0.01$). Afterward, the functional experiments demonstrated that the metastasis and viability of LC cells were suppressed by miR-30c-1-3p overexpression (Fig. 5C–E, $P < 0.01$).

MARCKSL1 is a Target Gene of miR-30c-1-3p

To explore the downstream regulatory mechanism of miR-30c-1-3p in LC, a total of 10 potential target genes (score > 95) was selected using miRDB software (Fig. 6A). MARCKSL1 was chosen in this study due to its high expression (Fig. 6B, $P < 0.01$; data from TCGA) in LC and poor prognosis for LC patients (Fig. 6C, logrank $P = 1.9 \times e^{-8}$). Figure 6D showed the binding site between miR-30c-1-3p and MARCKSL1. Afterward, DLR was conducted to verify the target relationship between them. As illustrated in Fig. 6E, a decreased luciferase activity was exhibited in the MARCKSL1 WT-miR-30c-1-3p mimics group compared to that of the MARCKSL1 WT-miR-NC group, while no statistical changes were observed in the MARCKSL1 MUT group ($P < 0.01$). We then determined the protein level of MARCKSL1 after transfection of miR-30c-1-3p mimics in A549 and H1299 cells. The results of western blot assay revealed that MARCKSL1 protein level was remarkably repressed by miR-30c-1-3p overexpression

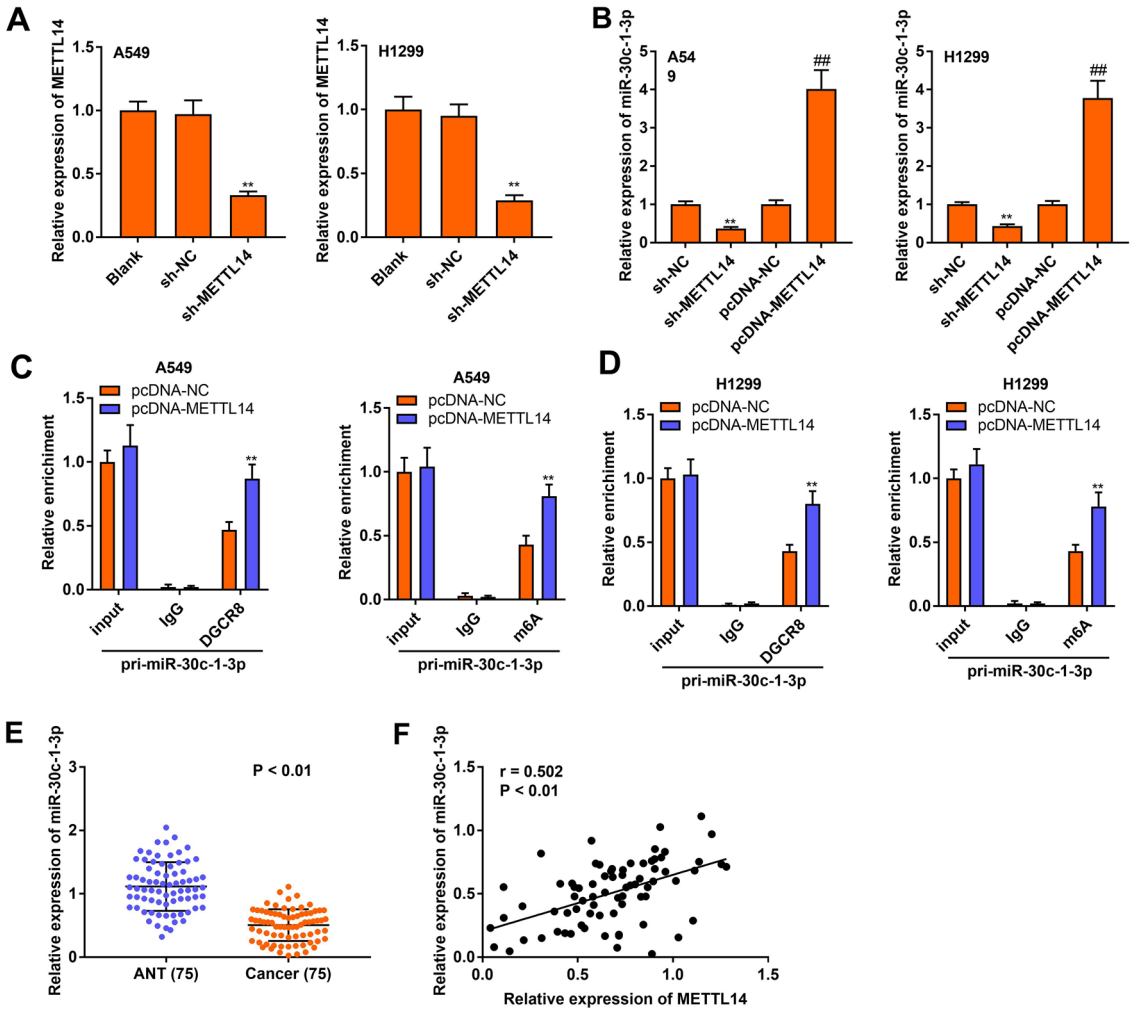

Fig. 4 METTL14-mediated m6A methylation regulates the processing of miR-30c-1-3p by DGCR8. **A** The expression of METTL14 in LC cells after transfection of sh-METTL14/NC was detected by qRT-PCR. $^{**}P<0.01$ vs. the sh-NC group. **B** The expression of miR-30c-1-3p in LC cells after transfection of sh-METTL14/NC or pcDNA-METTL14/NC was detected by qRT-PCR. $^{**}P<0.01$ vs. the sh-NC group, $^{\#\#}P<0.01$ vs. the pcDNA-NC group. **C** The m6A modification level of pri-miR-30c-1-3p in A549 cells after different treatments was determined by RIP and Me-RIP assays. $^{**}P<0.01$ vs. the pcDNA-NC group. **D** The m6A modification level of pri-miR-30c-1-3p in H1299 cells after different treatments was determined by RIP and Me-RIP assays. $^{**}P<0.01$ vs. the pcDNA-NC group. **E** The expression of miR-30c-1-3p in LC tissues ($n=75$) and adjacent normal tissues ($n=75$) was detected by qRT-PCR. $P<0.01$ vs. the adjacent normal tissues. **F** The correlation between the expression of METTL14 and miR-30c-1-3p in LC tissues was assessed by Pearson's correlation analysis. $P<0.01$, $r=0.505$

(Fig. 6F, P < 0.01). In addition, we further discovered a relatively high expression of MARCKSL1 in tumor tissues in comparison to that of ANT (Fig. 6G, P < 0.01), and there was a negative correlation between the expression of miR-30c-1-3p and MARCKSL1 (Fig. 6H; $P<0.01$, $r=-0.4578$).

The Overexpressed METTL14 Suppresses the Cell Viability and Metastasis of A549 Cells Through Mediating the miR-30c-1-3p/MARCKSL1 Axis

Finally, rescue experiments were performed to investigate the interactions among METTL14, miR-30c-1-3p, and MARCKSL1 in LC. We initially determined that MARCKSL1 protein level was elevated by transfection of pcDNA-MARCKSL1 (Fig. 7A, $P<0.01$). Meanwhile, we further found that the protein level of MARCKSL1 was significantly repressed by METTL14 overexpression (Fig. 7B, $P<0.01$), and this situation was reversed by downregulation of miR-30c-1-3p ($P<0.05$). As presented in Fig. 7C–E, the rescue experiments demonstrated that the inhibitory effects of pcDNA-METTL14 on cell metastasis and viability were rescued by transfection of miR-30c-1-3p inhibitor or pcDNA-MARCKSL1 ($P<0.05$).

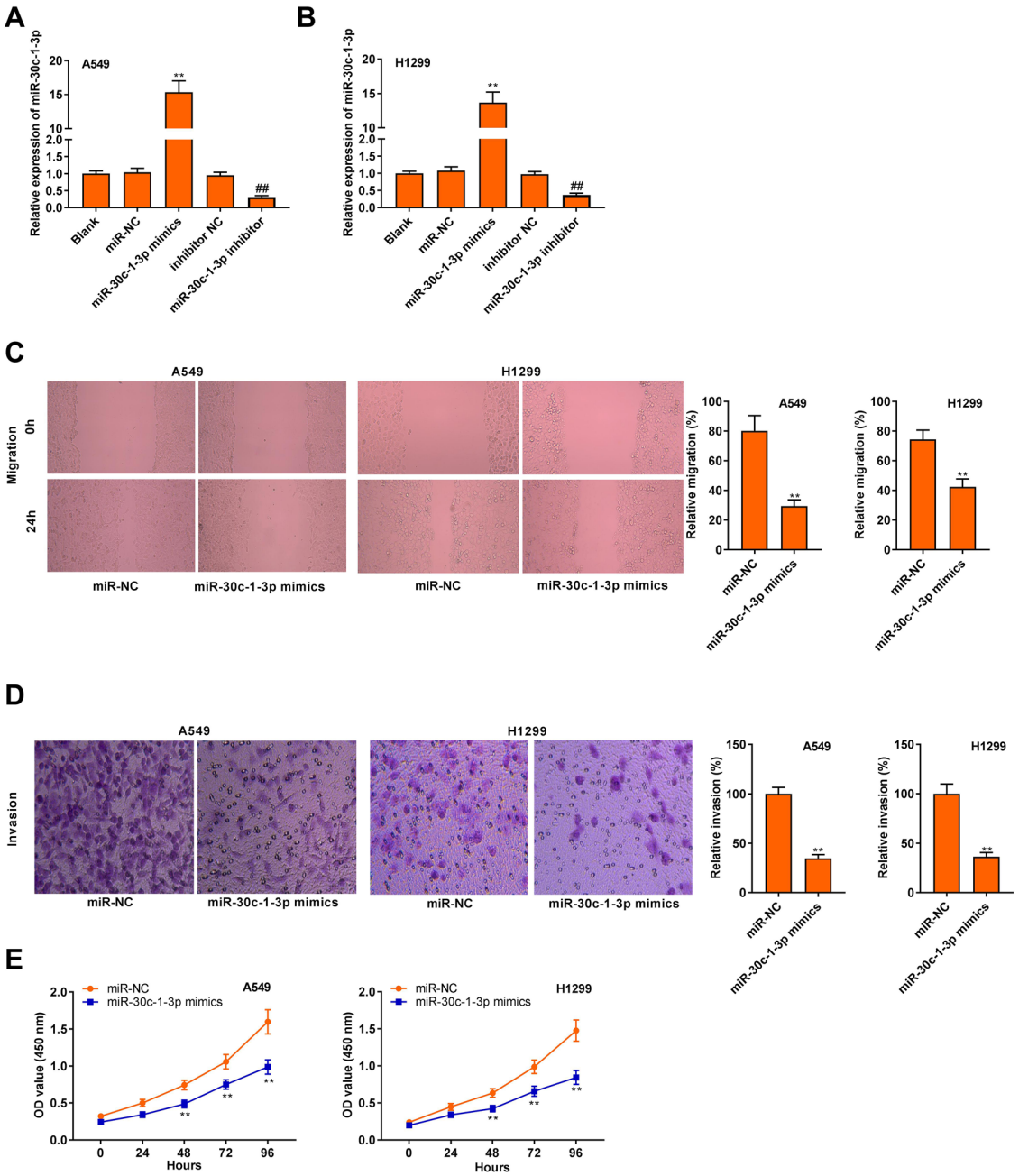

Fig. 5 Overexpression of miR-30c-1-3p inhibits the cell viability and metastasis in LC. **A** The expression of miR-30c-1-3p in A549 cells after transfection of miR-30c-1-3p mimics/miR-NC or miR-30c-1-3p inhibitor/inhibitor NC was detected by qRT-PCR. **B** The expression of miR-30c-1-3p in H1299 cells after transfection of miR-30c-1-3p mimics/miR-NC or miR-30c-1-3p inhibitor/inhibitor NC was detected by qRT-PCR. **C** The migration of LC cells was measured by wound healing assay. **D** The invasion of LC cells was measured by transwell assay. **E** The viability of LC was measured by MTT assay. $^{**}P < 0.01$ vs. the miR-NC group; $^{\#\#}P < 0.01$ vs. the inhibitor NC group

Discussion

Growing attention has been paid to the important role of m6A modification in carcinogenesis [12, 26, 27]. METTL14, a key RNA methyltransferase in the process of m6A modification, is reported to downregulate in tumor tissues compared to that of healthy controls [38, 41, 51]. Meanwhile, the overexpressed METTL14 represses the proliferation, migration, and invasion of cancer cells, such as HCC [38], CRC [41], and gastric cancer (GC) [51]. In the current study, low expression of METTL14 is not only identified in data analysis platform (TCGA and GEO), but also confirmed in LC clinical specimens and cell lines. Similarly, Li analyzed the expression levels of m6A methylation related regulators

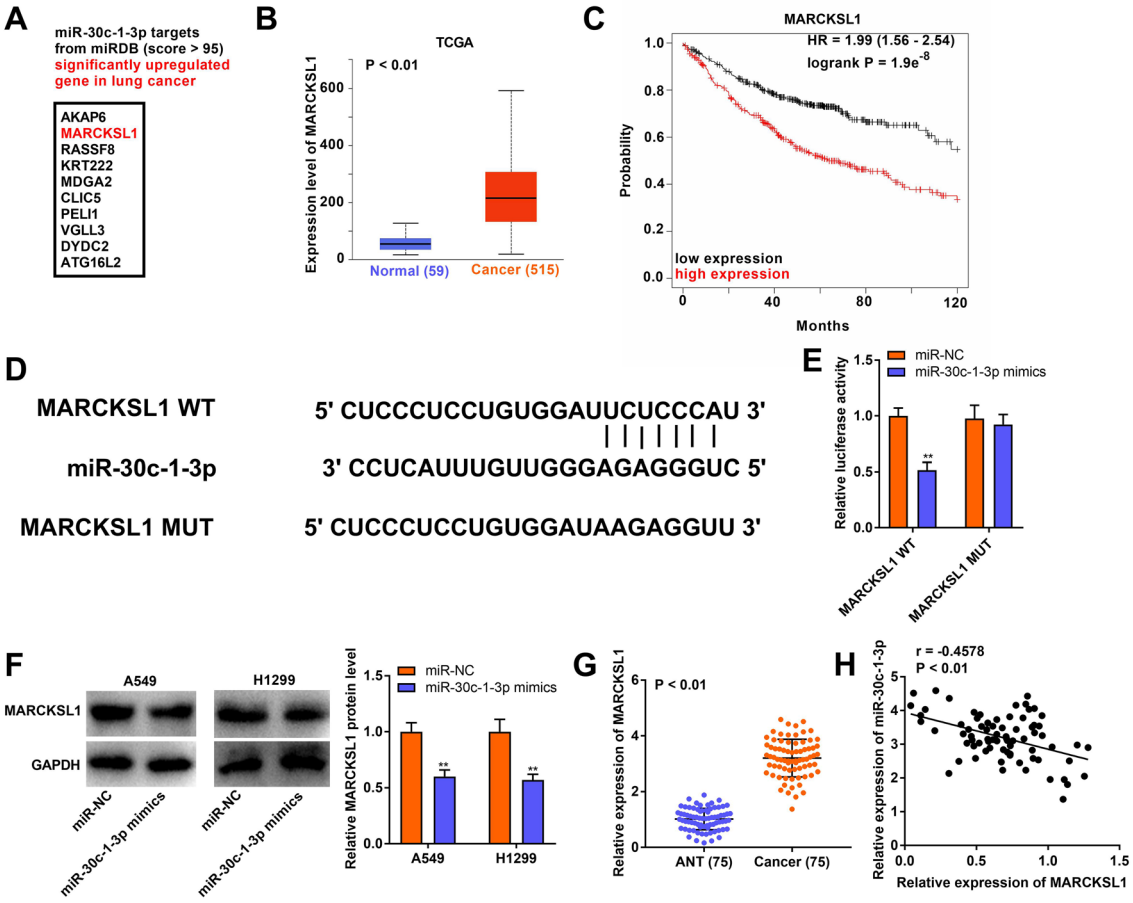

Fig. 6 MARCKSL1 is a target gene of miR-30c-1-3p. **A** Search for potential target genes of miR-30c-1-3p through the miRDB software. **B** The expression of MARCKSL1 in LC tissues was analyzed using TCGA database. $P<0.01$ vs. the normal tissues. **C** The effect of different expression level of MARCKSL1 on LC prognosis was analyzed using the platform of Kaplan–Meier Plotter. Logrank $P=1.9\times e^{-8}$. **D** The binding site between miR-30c-1-3p and MARCKSL1. **E** The luciferase activity in LC cells co-transfected with pGL3-MARCKSL1 WT/pGL3-MARCKSL1 MUT and miR-30c-1-3p mimics/miR-NC was determined by dual-luciferase reporter assay. **F** The protein level of MARCKSL1 in LC cells after transfection of miR-30c-1-3p/miR-NC was determined by western blot assay. **G** The expression of MARCKSL1 in LC tissues ($n=75$) and adjacent normal tissues ($n=75$) was detected by qRT-PCR. $P<0.01$ vs. the adjacent normal tissues. **H** The correlation between the expression of MARCKSL1 and miR-30c-1-3p in LC tissues was assessed by Pearson's correlation analysis. $P<0.01$, $r=-0.4578$

in LAD, and demonstrated that METTL14 expression is significantly decreased in the tumor tissues [35]. Additionally, we further found the cell viability and metastasis of LC cell lines (A549 and H1299) transfected with pcDNA-METTL14 were inhibited. Interestingly, overexpression of METTL14 also repressed the growth of tumor xenograft in a mouse model. Therefore, we speculated METTL14 may exhibit an anti-tumor role in the tumorigenesis of LC.

As a key mediator of m6A modification, METTL14 could modulate the half-life period of RNA, and control the pre-mRNA splicing, miRNA processing, nuclear export, and translation [10]. In addition, METTL14/m6A can process the pre-miRNA and accelerate its maturation through regulation of DGCR8 [38, 41, 42]. For instance, after recognition of DGCR, the processing effects of METTL14 on pre-miRNAs were confirmed, such as METTL14-pri-miR-126 in HCC [38], METTL14-pri-miR-375 in CRC [41], and METTL14-pri-miR-19a in AS [42] were confirmed. In this study, we initially searched 50 miRNAs in LinkedOmics databases that is positively correlated with METTL14. We speculated that METTL14 may be related to the maturation of these miRNAs. Our pre-experiments demonstrated that miR-30c-1-3p in the only one miRNA that is significantly downregulated by transfection of sh-METTL14, and is upregulated after transfection with pcDNA-METTL14. Given this, we believed that the maturation of miR-30c-1-3p may be mediated by METTL14. Furthermore, we found relatively high levels of pri-miR-30c-1-3p precipitated by DGCR8 and m6A antibodies upon METTL14 overexpression. The above results further validated our hypothesis.

We have demonstrated that METTL14 may be an anti-neoplastic factor existing in LC. So here comes the question:

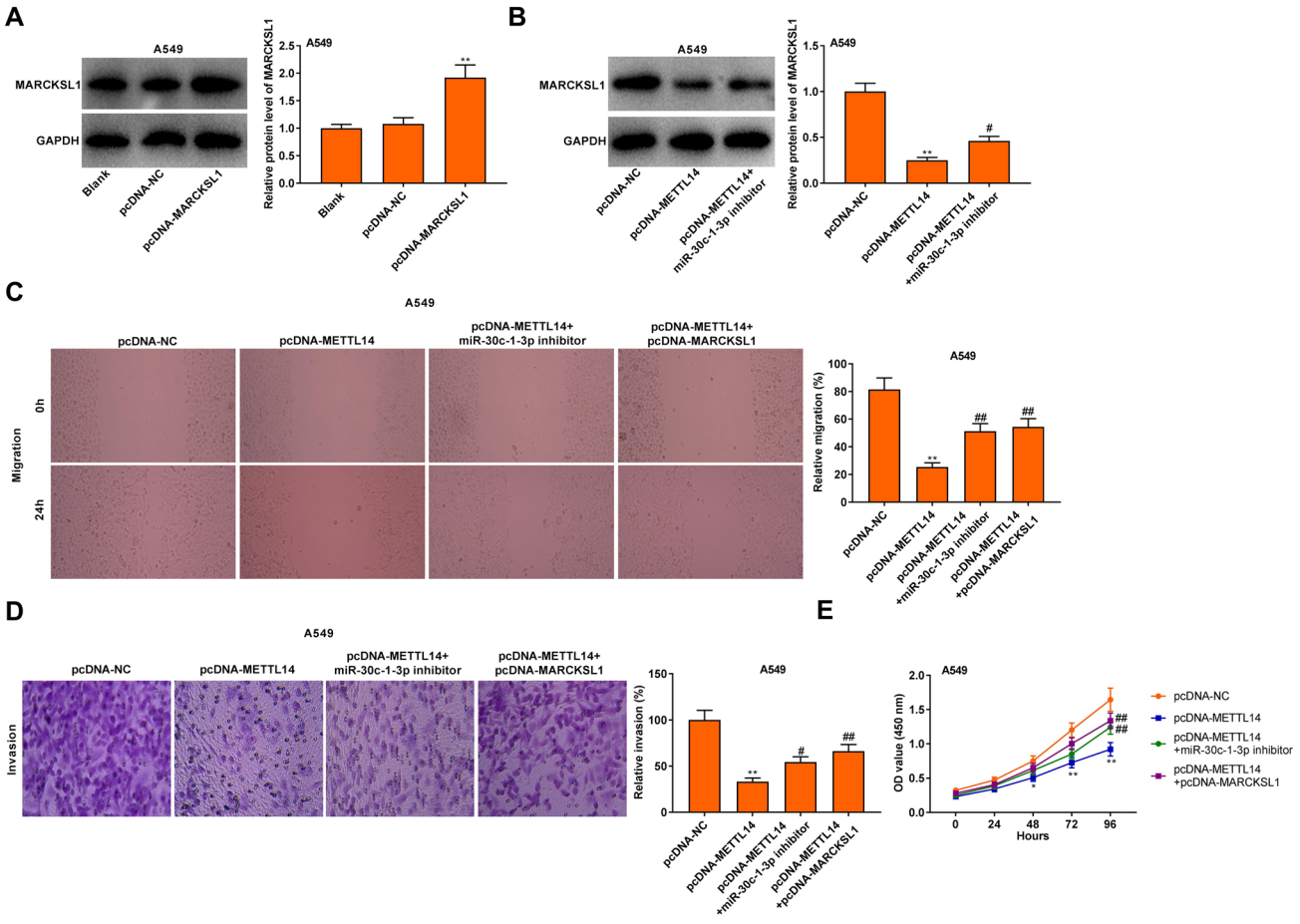

Fig. 7 The overexpressed METTL14 suppresses the cell viability and metastasis of A549 cells through mediating the miR-30c-1-3p/MARCKSL1 axis. **A** The protein level of MARCKSL1 in A549 cells after transfection of pcDNA-MARCKSL1/NC was determined by western blot assay. $^{**}P<0.01$ vs. the pcDNA-NC group. **B** The protein level of MARCKSL1 in A549 cells after transfection of pcDNA-METTL14, pcDNA-NC or pcDNA-METTL14 + miR-30c-1-3p inhibitor was determined by western blot assay. **C** The migration of LC cells was measured by wound healing assay. **D** The invasion of LC cells was measured by transwell assay. **E** The viability of LC was measured by MTT assay. $^{*}P<0.05$, $^{**}P<0.01$ vs. the pcDNA-NC group. $^{**}P<0.01$ vs. the pcDNA-NC group, $^{\#}P<0.05$, $^{\#\#}P<0.01$ the pcDNA-METTL14 group

whether the mature miR-30c-1-3p is associated with LC progression in case that the maturation of miR-30c-1-3p is mediated by METTL14. In fact, miR-30c-1-3p is well known as a suppressor in human cancers [43, 45]. Kordaß et al. revealed that miR-30c-1-3p represses the invasion of melanoma through regulation of invasion-related genes [43]. Chen et al. found a decreased miR-30c-1-3p in PC tissues, and miR-30c-1-3p overexpression contributes to inhibit the development of PC [45]. Interestingly, the expression of miR-30c-1-3p is also downregulated in LC tissues compared with ANT. At the same time, miR-30c-1-3p overexpression inhibited the cell viability and metastasis in LC. In addition, relatively low expression of miR-30c-1-3p reversed the inhibitory effects of overexpressed METTL14 on viability and metastasis of LC cells. Our results suggested that the mature miR-30c-1-3p modulated by METTL14/m6A was involved in the progression of LC.

MARCKSL1, a member of the myristoylated alanine-rich C kinase substrate (MARCKS) family, is reported to be implicated in the regulation of cancer growth and metastasis [47–49, 52]. For example, MARCKS targeted by miR-21 facilitates PC cell motility and invasion [47]. Overexpression MARCKS reversed the inhibiting effect of miR-34c-3p on osteosarcoma progression [49]. High expression of MARCKSL1 represents relatively poor prognosis for BRC patients [52], and miR-140-3p-MARCKSL1 axis leads to the inhibition of BRC cell cycle and migration [48]. Based on these previous results, we speculated MARCKSL1 may be modulated by the upstream miRNAs to affect cancer progression. In this study, we discovered that MARCKSL1 is upregulated in LC tissues, and is strong correlated with worse prognosis for LC patients, which was consistent with the previous results. Additionally, MARCKSL1 was identified as direct target of miR-30c-1-3p. The results implied

that the miR-30c-1-3p-MARCKSL1 axis may be crucial for the development of LC. As mentioned in the above discussion, we have demonstrated that METTL14 repressed LC progression through regulation of miR-30c-1-3p. Therefore, we further conjectured METTL14 ameliorated the malignant behaviors of LC via regulating the miR-30c-1-3p/MARCKSL1 axis. Subsequently, the results of feedback verification experiments showed that MARCKSL1 overexpression reversed the suppressive effects of METTL14 upregulation on cell viability and metastasis, which further confirmed our assumption. All the above results suggested that METTL14/m6A initially accelerated the maturation of miR-30c-1-3p and then mediated the expression of MARCKSL1 to suppress LC progression.

However, there were also some limitations in this study. First, our research mainly focused on the function of METTL14 in LC progression. Expression of other methyl transferase and demethylase associated with m6A modification from database analysis as well as in primary LC samples is absent. Second, the direct interaction of METTL14 with MARCKSL1 should be explored. We will consider elucidating these issues in future studies.

In summary, the current study uncovered that METTL14 shows anti-tumor role in LC. METTL14/m6A makes important contributions regarding the maturation of miR-30c-1-3p. More importantly, METTL14-mediated miR-30c-1-3p maturation represses the cell viability and metastasis in LC through regulation of MARCKSL1 expression. Our findings suggest that the METTL14-miR-30-1-3p-MARCKSL1 axis is crucial in the development of LC, providing an underlying therapeutic target for LC.

Supplementary Information The online version contains supplementary material available at https://doi.org/10.1007/s12033-021-00406-8.

Author Contributions Conceptualization: FL and YC; Methodology: W L; Formal analysis and investigation: FL, XH, and LW; Writing-original draft preparation: FL; Writing-review and editing: WL, YC, and JZ; Funding acquisition: FL; Resources: XH and LW; Supervision: YC.

Funding Not applicable.

Declarations

Conflict of interest The authors declare that they have no conflicts of interest.

Ethical Approval This study was performed in line with the principles of the Declaration of Helsinki. The present study was approved by Ethics Committee of Peoples Hospital of Rizhao, and the relevant informed consents were written by each patient.

Informed Consent Informed consent was obtained from all individual participants included in the study.

Consent to Publish Not applicable.

References

1. Travis, W. D. (2020). Lung cancer pathology: Current concepts. *Clinics in Chest Medicine, 41*(1), 67–85. https://doi.org/10.1016/j.ccm.2019.11.001
2. Siegel, R. L., Miller, K. D., & Jemal, A. (2019). Cancer statistics, 2019. *CA: A Cancer Journal for Clinicians, 69*(1), 7–34. https://doi.org/10.3322/caac.21551
3. Ridge, C. A., McErlean, A. M., & Ginsberg, M. S. (2013). Epidemiology of lung cancer. *Seminars in Interventional Radiology, 30*(2), 93–98. https://doi.org/10.1055/s-0033-1342949
4. Hussain, S. (2016). Nanomedicine for treatment of lung cancer. *Advances in Experimental Medicine and Biology, 890*, 137–147. https://doi.org/10.1007/978-3-319-24932-2_8
5. Quaratino, S., Forssmann, U., & Marschner, J. P. (2017). New approaches in immunotherapy for the treatment of lung cancer. *Current Topics in Microbiology and Immunology, 405*, 1–31. https://doi.org/10.1007/82_2014_428
6. Detterbeck, F. C., Boffa, D. J., Kim, A. W., & Tanoue, L. T. (2017). The Eighth Edition Lung Cancer Stage Classification. *Chest, 151*(1), 193–203. https://doi.org/10.1016/j.chest.2016.10.010
7. Cantara, W. A., Crain, P. F., Rozenski, J., McCloskey, J. A., Harris, K. A., Zhang, X., Vendeix, F. A., Fabris, D., & Agris, P. F. (2011). The RNA Modification Database, RNAMDB: 2011 update. *Nucleic Acids Research, 39*(Database Issue), D195-201. https://doi.org/10.1093/nar/gkq1028
8. Machnicka, M. A., Milanowska, K., Osman Oglou, O., Purta, E., Kurkowska, M., Olchowik, A., Januszewski, W., Kalinowski, S., Dunin-Horkawicz, S., Rother, K. M., Helm, M., Bujnicki, J. M., & Grosjean, H. (2013). MODOMICS: A database of RNA modification pathways—2013 Update. *Nucleic Acids Research, 41*(Database Issue), D262-267. https://doi.org/10.1093/nar/gks1007
9. Frye, M., Harada, B. T., Behm, M., & He, C. (2018). RNA modifications modulate gene expression during development. *Science, 361*(6409), 1346–1349. https://doi.org/10.1126/science.aau1646
10. Lee, M., Kim, B., & Kim, V. N. (2014). Emerging roles of RNA modification: m(6)A and U-tail. *Cell, 158*(5), 980–987. https://doi.org/10.1016/j.cell.2014.08.005
11. Gu, C., Wang, Z., Zhou, N., Li, G., Kou, Y., Luo, Y., Wang, Y., Yang, J., & Tian, F. (2019). Mettl14 inhibits bladder TIC self-renewal and bladder tumorigenesis through N(6)-methyladenosine of Notch1. *Molecular Cancer, 18*(1), 168. https://doi.org/10.1186/s12943-019-1084-1
12. Jin, D., Guo, J., Wu, Y., Du, J., Yang, L., Wang, X., Di, W., Hu, B., An, J., Kong, L., Pan, L., & Su, G. (2019). m(6)A mRNA methylation initiated by METTL3 directly promotes YAP translation and increases YAP activity by regulating the MALAT1-miR-1914-3p-YAP axis to induce NSCLC drug resistance and metastasis. *Journal of Hematology and Oncology, 12*(1), 135. https://doi.org/10.1186/s13045-019-0830-6
13. Qian, J. Y., Gao, J., Sun, X., Cao, M. D., Shi, L., Xia, T. S., Zhou, W. B., Wang, S., Ding, Q., & Wei, J. F. (2019). KIAA1429 acts as an oncogenic factor in breast cancer by regulating CDK1 in an N6-methyladenosine-independent manner. *Oncogene, 38*(33), 6123–6141. https://doi.org/10.1038/s41388-019-0861-z
14. Selberg, S., Blokhina, D., Aatonen, M., Koivisto, P., Siltanen, A., Mervaala, E., Kankuri, E., & Karelson, M. (2019). Discovery of small molecules that activate RNA methylation through cooperative binding to the METTL3-14-WTAP complex active site. *Cell Reports, 26*(13), 3762-3771.e3765. https://doi.org/10.1016/j.celrep.2019.02.100
15. Zhang, S., Zhao, B. S., Zhou, A., Lin, K., Zheng, S., Lu, Z., Chen, Y., Sulman, E. P., Xie, K., Bogler, O., Majumder, S., He, C., &

Huang, S. (2017). m(6)A demethylase ALKBH5 maintains tumorigenicity of glioblastoma stem-like cells by sustaining FOXM1 expression and cell proliferation program. *Cancer Cell, 31*(4), 591-606.e596. https://doi.org/10.1016/j.ccell.2017.02.013

16. Li, Z., Weng, H., Su, R., Weng, X., Zuo, Z., Li, C., Huang, H., Nachtergaele, S., Dong, L., Hu, C., Qin, X., Tang, L., Wang, Y., Hong, G. M., Wang, X., Chen, P., Gurbuxani, S., Arnovitz, S., Li, Y., Li, S., et al. (2017). FTO plays an oncogenic role in acute myeloid leukemia as a N(6)-methyladenosine RNA demethylase. *Cancer Cell, 31*(1), 127–141. https://doi.org/10.1016/j.ccell.2016.11.017
17. Tiwari, N., Tiwari, V. K., Waldmeier, L., Balwierz, P. J., Arnold, P., Pachkov, M., Meyer-Schaller, N., Schubeler, D., van Nimwegen, E., & Christofori, G. (2013). Sox4 is a master regulator of epithelial–mesenchymal transition by controlling Ezh2 expression and epigenetic reprogramming. *Cancer Cell, 23*(6), 768–783. https://doi.org/10.1016/j.ccr.2013.04.020
18. Huang, H., Weng, H., Sun, W., Qin, X., Shi, H., Wu, H., Zhao, B. S., Mesquita, A., Liu, C., Yuan, C. L., Hu, Y. C., Huttelmaier, S., Skibbe, J. R., Su, R., Deng, X., Dong, L., Sun, M., Li, C., Nachtergaele, S., Wang, Y., et al. (2018). Recognition of RNA N(6)-methyladenosine by IGF2BP proteins enhances mRNA stability and translation. *Nature Cell Biology, 20*(3), 285–295. https://doi.org/10.1038/s41556-018-0045-z
19. Zhao, B. S., Wang, X., Beadell, A. V., Lu, Z., Shi, H., Kuuspalu, A., Ho, R. K., & He, C. (2017). m(6)A-dependent maternal mRNA clearance facilitates zebrafish maternal-to-zygotic transition. *Nature, 542*(7642), 475–478. https://doi.org/10.1038/nature21355
20. Lin, Z., Hsu, P. J., Xing, X., Fang, J., Lu, Z., Zou, Q., Zhang, K. J., Zhang, X., Zhou, Y., Zhang, T., Zhang, Y., Song, W., Jia, G., Yang, X., He, C., & Tong, M. H. (2017). Mettl3-/Mettl14-mediated mRNA N(6)-methyladenosine modulates murine spermatogenesis. *Cell Research, 27*(10), 1216–1230. https://doi.org/10.1038/cr.2017.117
21. Wen, J., Lv, R., Ma, H., Shen, H., He, C., Wang, J., Jiao, F., Liu, H., Yang, P., Tan, L., Lan, F., Shi, Y. G., Shi, Y., & Diao, J. (2018). Zc3h13 regulates nuclear RNA m(6)A methylation and mouse embryonic stem cell self-renewal. *Molecular Cell, 69*(6), 1028-1038.e1026. https://doi.org/10.1016/j.molcel.2018.02.015
22. Fustin, J. M., Doi, M., Yamaguchi, Y., Hida, H., Nishimura, S., Yoshida, M., Isagawa, T., Morioka, M. S., Kakeya, H., Manabe, I., & Okamura, H. (2013). RNA-methylation-dependent RNA processing controls the speed of the circadian clock. *Cell, 155*(4), 793–806. https://doi.org/10.1016/j.cell.2013.10.026
23. Xiang, Y., Laurent, B., Hsu, C. H., Nachtergaele, S., Lu, Z., Sheng, W., Xu, C., Chen, H., Ouyang, J., Wang, S., Ling, D., Hsu, P. H., Zou, L., Jambhekar, A., He, C., & Shi, Y. (2017). RNA m(6)A methylation regulates the ultraviolet-induced DNA damage response. *Nature, 543*(7646), 573–576. https://doi.org/10.1038/nature21671
24. Zhang, C., Chen, Y., Sun, B., Wang, L., Yang, Y., Ma, D., Lv, J., Heng, J., Ding, Y., Xue, Y., Lu, X., Xiao, W., Yang, Y. G., & Liu, F. (2017). m(6)A modulates haematopoietic stem and progenitor cell specification. *Nature, 549*(7671), 273–276. https://doi.org/10.1038/nature23883
25. Li, H. B., Tong, J., Zhu, S., Batista, P. J., Duffy, E. E., Zhao, J., Bailis, W., Cao, G., Kroehling, L., Chen, Y., Wang, G., Broughton, J. P., Chen, Y. G., Kluger, Y., Simon, M. D., Chang, H. Y., Yin, Z., & Flavell, R. A. (2017). m(6)A mRNA methylation controls T cell homeostasis by targeting the IL-7/STAT5/SOCS pathways. *Nature, 548*(7667), 338–342. https://doi.org/10.1038/nature23450
26. Du, C., Lv, C., Feng, Y., & Yu, S. (2020). Activation of the KDM5A/miRNA-495/YTHDF2/m6A-MOB3B axis facilitates prostate cancer progression. *Journal of Experimental and Clinical Cancer Research, 39*(1), 223. https://doi.org/10.1186/s13046-020-01735-3
27. Strick, A., von Hagen, F., Gundert, L., Klumper, N., Tolkach, Y., Schmidt, D., Kristiansen, G., Toma, M., Ritter, M., & Ellinger, J. (2020). The N(6)-methyladenosine (m(6) A) erasers alkylation repair homologue 5 (ALKBH5) and fat mass and obesity-associated protein (FTO) are prognostic biomarkers in patients with clear cell renal carcinoma. *BJU International, 125*(4), 617–624. https://doi.org/10.1111/bju.15019
28. Lin, S., Choe, J., Du, P., Triboulet, R., & Gregory, R. I. (2016). The m(6)A methyltransferase METTL3 promotes translation in human cancer cells. *Molecular Cell, 62*(3), 335–345. https://doi.org/10.1016/j.molcel.2016.03.021
29. Weng, L., Qiu, K., Gao, W., Shi, C., & Shu, F. (2020). LncRNA PCGEM1 accelerates non-small cell lung cancer progression via sponging miR-433-3p to upregulate WTAP. *BMC Pulmonary Medicine, 20*(1), 213. https://doi.org/10.1186/s12890-020-01240-5
30. Wang, H., Zhao, X., & Lu, Z. (2021). m(6)A RNA methylation regulators act as potential prognostic biomarkers in lung adenocarcinoma. *Frontiers in Genetics, 12*, 622233. https://doi.org/10.3389/fgene.2021.622233
31. Zhu, Z., Qian, Q., Zhao, X., Ma, L., & Chen, P. (2020). N(6)-methyladenosine ALKBH5 promotes non-small cell lung cancer progress by regulating TIMP3 stability. *Gene, 731*, 144348. https://doi.org/10.1016/j.gene.2020.144348
32. Li, J., Han, Y., Zhang, H., Qian, Z., Jia, W., Gao, Y., Zheng, H., & Li, B. (2019). The m6A demethylase FTO promotes the growth of lung cancer cells by regulating the m6A level of USP7 mRNA. *Biochemical and Biophysical Research Communications, 512*(3), 479–485. https://doi.org/10.1016/j.bbrc.2019.03.093
33. Zhang, Y., Liu, X., Liu, L., Li, J., Hu, Q., & Sun, R. (2020). Expression and prognostic significance of m6A-related genes in lung adenocarcinoma. *Medical Science Monitor, 26*, e919644. https://doi.org/10.12659/MSM.919644
34. Chen, X., Xu, M., Xu, X., Zeng, K., Liu, X., Pan, B., Li, C., Sun, L., Qin, J., Xu, T., He, B., Pan, Y., Sun, H., & Wang, S. (2020). METTL14-mediated N6-methyladenosine modification of SOX4 mRNA inhibits tumor metastasis in colorectal cancer. *Molecular Cancer, 19*(1), 106. https://doi.org/10.1186/s12943-020-01220-7
35. Li, F., Wang, H., Huang, H., Zhang, L., Wang, D., & Wan, Y. (2020). m6A RNA methylation regulators participate in the malignant progression and have clinical prognostic value in lung adenocarcinoma. *Frontiers in Genetics, 11*, 994. https://doi.org/10.3389/fgene.2020.00994
36. Guo, H., Ingolia, N. T., Weissman, J. S., & Bartel, D. P. (2010). Mammalian microRNAs predominantly act to decrease target mRNA levels. *Nature, 466*(7308), 835–840. https://doi.org/10.1038/nature09267
37. Cai, X., Wang, X., Cao, C., Gao, Y., Zhang, S., Yang, Z., Liu, Y., Zhang, X., Zhang, W., & Ye, L. (2018). HBXIP-elevated methyltransferase METTL3 promotes the progression of breast cancer via inhibiting tumor suppressor let-7g. *Cancer Letters, 415*, 11–19. https://doi.org/10.1016/j.canlet.2017.11.018
38. Ma, J. Z., Yang, F., Zhou, C. C., Liu, F., Yuan, J. H., Wang, F., Wang, T. T., Xu, Q. G., Zhou, W. P., & Sun, S. H. (2017). METTL14 suppresses the metastatic potential of hepatocellular carcinoma by modulating N(6)-methyladenosine-dependent primary microRNA processing. *Hepatology, 65*(2), 529–543. https://doi.org/10.1002/hep.28885
39. Yi, D., Wang, R., Shi, X., Xu, L., Yilihamu, Y., & Sang, J. (2020). METTL14 promotes the migration and invasion of breast cancer cells by modulating N6methyladenosine and hsamiR146a5p expression. *Oncology Reports, 43*(5), 1375–1386. https://doi.org/10.3892/or.2020.7515

40. Bi, X., Lv, X., Liu, D., Guo, H., Yao, G., Wang, L., Liang, X., & Yang, Y. (2020). METTL3-mediated maturation of miR-126-5p promotes ovarian cancer progression via PTEN-mediated PI3K/Akt/mTOR pathway. *Cancer Gene Therapy*. https://doi.org/10.1038/s41417-020-00222-3
41. Chen, X., Xu, M., Xu, X., Zeng, K., Liu, X., Sun, L., Pan, B., He, B., Pan, Y., Sun, H., Xia, X., & Wang, S. (2020). METTL14 suppresses CRC progression via regulating N6-methyladenosine-dependent primary miR-375 processing. *Molecular Therapy, 28*(2), 599–612. https://doi.org/10.1016/j.ymthe.2019.11.016
42. Zhang, B. Y., Han, L., Tang, Y. F., Zhang, G. X., Fan, X. L., Zhang, J. J., Xue, Q., & Xu, Z. Y. (2020). METTL14 regulates M6A methylation-modified primary miR-19a to promote cardiovascular endothelial cell proliferation and invasion. *European Review for Medical and Pharmacological Sciences, 24*(12), 7015–7023. https://doi.org/10.26355/eurrev_202006_21694
43. Kordass, T., Weber, C. E. M., Eisel, D., Pane, A. A., Osen, W., & Eichmuller, S. B. (2018). miR-193b and miR-30c-1(*) inhibit, whereas miR-576-5p enhances melanoma cell invasion in vitro. *Oncotarget, 9*(65), 32507–32522. https://doi.org/10.18632/oncotarget.25986
44. Zhang, X., Zhang, G., Huang, H., Li, H., Lin, S., & Wang, Y. (2020). Differentially expressed microRNAs in radioresistant and radiosensitive atypical meningioma: A clinical study in Chinese patients. *Frontiers in Oncology, 10*, 501. https://doi.org/10.3389/fonc.2020.00501
45. Chen, W., Yao, G., & Zhou, K. (2019). miR-103a-2-5p/miR-30c-1-3p inhibits the progression of prostate cancer resistance to androgen ablation therapy via targeting androgen receptor variant 7. *Journal of Cellular Biochemistry, 120*(8), 14055–14064. https://doi.org/10.1002/jcb.28680
46. Wu, M., Liang, G., Duan, H., Yang, X., Qin, G., & Sang, N. (2019). Synergistic effects of sulfur dioxide and polycyclic aromatic hydrocarbons on pulmonary pro-fibrosis via mir-30c-1-3p/transforming growth factor beta type II receptor axis. *Chemosphere, 219*, 268–276. https://doi.org/10.1016/j.chemosphere.2018.12.016
47. Li, T., Li, D., Sha, J., Sun, P., & Huang, Y. (2009). MicroRNA-21 directly targets MARCKS and promotes apoptosis resistance and invasion in prostate cancer cells. *Biochemical and Biophysical Research Communications, 383*(3), 280–285. https://doi.org/10.1016/j.bbrc.2009.03.077
48. Salem, O., Erdem, N., Jung, J., Munstermann, E., Worner, A., Wilhelm, H., Wiemann, S., & Korner, C. (2016). The highly expressed 5′isomiR of hsa-miR-140-3p contributes to the tumor-suppressive effects of miR-140 by reducing breast cancer proliferation and migration. *BMC Genomics, 17*, 566. https://doi.org/10.1186/s12864-016-2869-x
49. Liu, H., Su, P., Zhi, L., & Zhao, K. (2017). miR34c3p acts as a tumor suppressor gene in osteosarcoma by targeting MARCKS. *Molecular Medicine Reports, 15*(3), 1204–1210. https://doi.org/10.3892/mmr.2017.6108
50. Liang, W., Gao, R., Yang, M., Wang, X., Cheng, K., Shi, X., He, C., Li, Y., Wu, Y., Shi, L., Chen, J., & Yu, X. (2020). MARCKSL1 promotes the proliferation, migration and invasion of lung adenocarcinoma cells. *Oncology Letters, 19*(3), 2272–2280. https://doi.org/10.3892/ol.2020.11313
51. Liu, X., Xiao, M., Zhang, L., Li, L., Zhu, G., Shen, E., Lv, M., Lu, X., & Sun, Z. (2020). The m6A methyltransferase METTL14 inhibits the proliferation, migration, and invasion of gastric cancer by regulating the PI3K/AKT/mTOR signaling pathway. *Journal of Clinical Laboratory Analysis*. https://doi.org/10.1002/jcla.23655
52. Jonsdottir, K., Zhang, H., Jhagroe, D., Skaland, I., Slewa, A., Bjorkblom, B., Coffey, E. T., Gudlaugsson, E., Smaaland, R., Janssen, E. A., & Baak, J. P. (2012). The prognostic value of MARCKS-like 1 in lymph node-negative breast cancer. *Breast Cancer Research Treatment, 135*(2), 381–390. https://doi.org/10.1007/s10549-012-2155-9